PCCP

Accepted Manuscript

ROYAL SOCIETY OF CHEMISTRY

www.rsc.org/pccp

Journal Name

RSCPublishing

COMMUNICATION

Electronic structure variation at the surface and bulk of $LiNi_{0.5}Mn_{1.5}O_4$ cathode as a function of state of charge: X-ray absorption spectroscopic study

Cite this: DOI: 10.1039/xoxxoooooox

Received ooth January 2012,
Accepted ooth January 2012

DOI: 10.1039/xoxxoooooox

www.rsc.org/

Jigang Zhou[a,c]* , Da Hong[b], Jian Wang[a], Yongfeng Hu[a], Xiaohua Xie[d] , Haitao Fang[b]*

The electronic structure at Ni, Mn and O sites and their evolution upon electrochemical lithiation of $Li_{1-x}Ni_{0.5}Mn_{1.5}O_4$ in a lithium ion battery has been explored using comprehensive X-ray absorption near edge spectroscopy (XANES) at Ni and Mn $L_{3,2}$- and O K-edges with both surface sensitive and bulk sensitive detections. It has confirmed that Ni reduction from Ni^{4+} to Ni^{2+} plays the leading role in charge compensation when the lithiation is above 4.5 V. Our study also unveils the participation of oxygen in the charge compensation. Furthermore, the enhanced difference in electronic structure between surface and bulk in electrochemically cycled samples and different surface electronic structure between fully discharged LNMO and pristine one highlight importance of electrochemical activation. These findings are critical for a better understanding of the electrochemical reaction of LNMO and the influence of structural modifications in surface region on its performance, and then will assist further effort to improve this high voltage cathode material for its application in lithium ion battery.

High-voltage spinel $LiNi_{0.5}Mn_{1.5}O_4$ (LNMO) affords a cost-effective way to improve the energy density of lithium ion battery since it has a 4.7 V charge-discharge plateau due to the Ni^{4+}/Ni^{3+} and Ni^{3+}/Ni^{2+} redox couples[1]. The three dimensional lithium diffusion paths in the spinel structure also grant it a high rate-capacity which is characteristic of high power electrode. The unique combination of high energy and power density in this material makes it one of most promising candidates for batteries in electric-drive vehicles[1]. However, issues involving the stability of electrolyte at high voltage, and the performance dependence on the structural ordering, doping/substitution and impurity are still not completely understood[2-4]. For instance, the role of Mn^{3+} in LNMO performance, activation, rate capacity[3] or instability[5], still need to be further studied., The surface chemistry of LNMO can be designed to be different from that of the bulk (crystallinity and/or composition) [2]. In addition to the complicated chemistry in LNMO and its application in a battery, the electronic structure of this material is also worthy exploring since electronic structure, including valence, spin and covalence, dictates electron conductivity, ion diffusion and structural stability and phase transformation, which are key factors for its electrochemical performance[6, 7]. For instance, the Ni^{4+}/Ni^{3+} and Ni^{3+}/Ni^{2+} redox couples in LNMO can be accessed in a voltage plateau without a voltage step when the Fermi energy of cathode is "pinned" at the top of the O p bands.[1, 8] It is generally accepted that the discharge voltage plateau at 4.7V is due to Ni^{4+}/Ni^{2+} redox and the 4.1V step is due to the reaction of Mn^{4+}/Mn^{3+} [1]. But the solid evidence of these two steps and the clear understanding of roles by oxygen and Mn in this process are still elusive. Nor is it clear if there is any difference in the electronic structure between surface and bulk and how this difference affects the stability and rate performance of LNMO and electrolyte stability. All of these issues point out that tracking structural change at transition metals (Ni and Mn) and O sites in LNMO upon (de)lithiations with both surface and bulk detections is important for a full understanding of the electrochemical process. X-ray absorption near edge structure (XANES) spectroscopy deals with the measurement and interpretation of the photoabsorption cross-section variation across a particular core level (absorption edge) of an atom in a chemical environment up to ~50 eV above the threshold. The absorption features in XANES track bound to bound and bound to quasi-bound (multiple scattering) transitions thus affording element specificity and local chemical environment sensitivity. XANES has been applied to reveal the fundamental structure and bonding in lithium ion battery electrode materials[9] and their change under different

states of charge (SOC, a function of Li concentration in the host) [6, 7, 10-15]. Transition metal $L_{3,2}$-edge can directly probe the oxidation state, spin state and covalence of metal oxide especially when combined with the O K-edge spectrum[16, 17], therefore they are very powerful in exploring the critical electronic structure around Fermi level for battery electrode materials. More importantly, XANES in the soft X-ray range can simultaneously access surface and bulk of the sample via total electron yield and fluorescence yield, respectively. This letter reports an application of Ni and Mn $L_{3,2}$-edges and O K-edge XANES to study the structure in LNMO and its evolution along lithiation to afford a deeper understanding of the lithiation process and roles of each element in the process.

LNMO powder (500 nm spinel particle aggregates into secondary micrometer-sized particles, inset of Figure 1a) was purchased from Hunan Shanshan Co. Electrodes were prepared by casting a slurry of the LNMO 80wt%, super P (Timcal) 10wt%, and polyvinylidene fluoride (PVDF, Alfa Aesar) 10wt%, in an *N* -methyl pyrrolidone (NMP, Alfa Aesar) slurry onto aluminium foil. After the slurry was dried at 50 ^{o}C, the electrodes were punched into 15.5 cm ø disks. The active material loading was 2.0-2.3 mg/cm^2 weight and 15±2 µm thick. The coin cells were assembled in argon-filled glove-box with the thus fabricated cathodes, lithium foil anode, 1 M $LiPF_6$ in ethylene carbonate/ dimethyl carbonate (EC/DMC) electrolyte (Novolyte Tech, Suzhou), and Celgard M824 separator. In order to obtain stable performance of each cell, the cell was fully charged to 5.2 V and discharged to 3 V for 5 cycles at 1 C, and then discharged 0%, 20%, 40%, 60%, 80% and 100% of their stable discharge capacities to get different state of charge (SOC) in the 6th cycle. The cycling voltage profiles are displayed in Figure 1b. At each SOC, the coin cell was disassembled and the electrode washed by DMC for 3 times. All electrodes were dried in the glove box and sealed in Al foil bag under Ar and transported into test instruments quickly to avoid contamination effects of ambient environment.. Though the current method can minimize the possible surface structure change future in situ or operando measurement is much more desirable and will be pursued in the future. The XANES experiment of pristine and cycled LNMO with different SOC was performed at the SGM beamline in a vacuum chamber at ~10^{-8} torr and data was recorded in the surface sensitive total electron yield (TEY, sensitive to the top ~ 5-10 nm) and bulk sensitive fulorence yield (FY, ~ 100 nm). Due to the self absorption distortion, FY at Mn $L_{3,2}$-edge cannot be properly measured. Alternatively, Inverse Partial Fluorecence Yield (IPFY) was used by monitoring the inverse of O K-edge fluorecence yield to access the "bulk" sensitive Mn $L_{3,2}$-edge spectrum for the fluorecence mode[18]. XANES data were first normalized to the incident photon flux I_0 measured with a fresh gold mesh located upstream of the sample. After background correction, the XANES was normalized to the edge jump (the difference in absorption just below and at a flat region above the edge).

The charge-discharge profiles in Fig. 1b show distinct performance in the first charge-discharge cycle relative to the subsequent cycles in terms of : 1) a small charge plateau at ~ 3V; 2) much lower Coulomb efficiency in the first cycle which is related to the formation of solid electrolyte interphase (SEI) layer, a Li permeable passivation layer, in the first charge[1]; and 3) gradual voltage decrease with a slope at the end of first discharge and this voltage drop becomes more sharp in subsequent cycles. The last point reflects the kinetic difference of lithiation process in different cycles. In addition to a voltage plateau at 4.7 V, a discharge step at 4 V is visible which shall be caused by Mn^{4+} to Mn^{3+} redox reaction[1]. Interestingly, this voltage step almost disappears in charge profile which indicates the possibility of disproportion reaction of Mn^{3+} at the end of discharge which decomposes Mn^{3+} into soluble Mn^{2+} and Mn^{4+}.[1, 5] The detailed electronic structure evolution during the lithiation process will be explored by XANES in Ni, Mn and O sites in following sections.

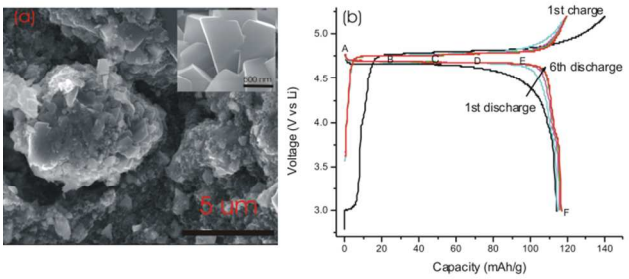

Fig. 1 (a) SEM image of the LNMO electrode and pristine spinel LNMO particles (a, inset); and (b) charge and discharge profiles for the first 6 cycles of LNMO electrode. At the 6th discharge, samples of A, B, C, D, E, and F with different SOCs (100%, 80%, 60%, 40%, 20% and 0%, respectively) were obtained.

We will focus first on the Ni $L_{3,2}$-edge XANES of LNMO with different SOCs to explore the electronic structure at Ni site upon electrochemical (de)lithiation. Both "bulk" sensitive FY mode with a probe depth of ~ 100 nm and surface sensitive TEY mode with a probe depth of ~ 5 nm were used to collect Ni $L_{3,2}$-edge XANES and the spectra are displayed in Fig. 2a and 2b, respectively. The $L_{3,2}$-edges of 3d transition metals result from the electronic transitions from the metal 2p level to mostly unoccupied 3d states which are sensitive to the oxidation, spin state and covalence[7, 17]. $L_{3,2}$-edge spectra consist of L_3-edge (from Ni $2p_{3/2}$ to Ni 3d state) and L_2-edge (from Ni $2p_{1/2}$ to Ni 3d state), with L_3-edge normally presenting more features due to the ligand field splitting effect. The electronic structure change among LNMO with different SOCs is apprent in Fig. 2a. The pristine and LNMO samples with low SOCs (E and F) are comparable to the low spin Ni^{2+} ($t_{2g}^6e_g^2$)[9, 19], while LNMO samples with high SOCs clearly present new features. Starting from the LNMO with SOC of 40% (sample D), peak 2 around 854 eV becomes more intense and shifts to lower energy. This shift becomes very clear in LNMO with a SOC of 60% (sample C) where the peak 2 moves to ~853.6 eV with an intensity higher than that of the peak 3 at 852.8 eV. We assume spectroscopic features in sample C corresponding to the Ni^{3+} with low spin state ($t_{2g}^6e_g^1$). With even higher SOC of 80% (sample B), a new feature, peak 1 at ~ 855.2 eV evolves and becoming dominat in LNMO with SOC of 100% (sample A). This new feature can be assigned to the low spin Ni^{4+} ($t_{2g}^6e_g^0$). At a probe depth of 100 nm, the Ni $L_{3,2}$-edge FY spectra thus clearly show that the transition of Ni^{4+} to Ni^{2+} via a intermediate state of Ni^{3+} corresponding to the charge compensation process when the electrode was discharged from 100% SOC (A) to 20 % SOC (E).

Though the lithiation definitely happen from E to F, the Ni redox does not appear to be involved in this discharge period since there is almost no change in Ni L-edge spectra between those two states[1]. When we turn our attention to the surface sensitive TEY spectra shown in Fig. 2b, we can observe substantial spectral difference with lower intensities of peaks 1 and 2 relative to that of peak 3, as compared to the FY case. Such difference is more obvious in higher SOC samples (A, B, and C). This clearly displays the structural difference between the surface and "bulk" which has also been observed in other transition metal oxide cathodes[12]. Such spectral difference could mean that there is more Ni with lower oxidation state at the surface than that in the "bulk". Such phenomena have been observed in other metal oxide cathodes[6, 14, 20] and it might mean a Li enriched surface considering the higher charging/discharging rate (1C) used in this study. It should be noted that LNMO at higher voltage during the first cycle can oxidize the electrolyte to form a SEI, which shall possibly in turn reduce the surface Ni species and bring Li ion back to the surface region of LNMO. Surface chemistry in cycled LNMO is very complex and dynamic, for instance, SEI stripping has been confirmed by in situ FTIR during discharge[21] which hints gradually changed LNMO surface structure in first several electrochemical cycles. Further systematic studies are necessary to clarify the real cause of the surface Ni reduction but the lower oxidation states of Ni shall be beneficial for the stabilization of electrolyte due to a lower surface potential.

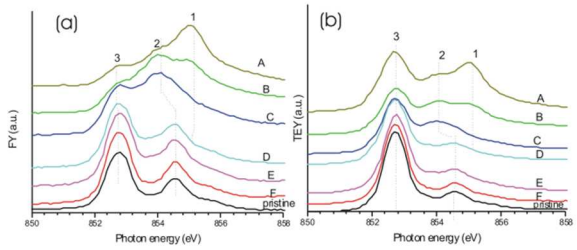

Fig. 2 XANES of LNMO with different SOC and pristine LNMO at Ni L_3-edge recorded in FY mode (a), and recorded at TEY mode (b).

The electronic evolution during (de)lithiation in LNMO was further studied by Mn L_3-edge XANES at IPFY and TEY modes as shown in Fig 3. Similar to the Ni case, Mn L_3 edge involves the electronic transition from Mn $2p_{3/2}$ to Mn 3d state and it is sensitive to the Mn 3d state (oxidation state, spin and colvalence). All spectra have similar feature (peaks of 1, 2 and 3) and comparable to Mn^{4+},[12, 13] especially in the bulk sensitive IPFY (Fig. 3a). This agrees with theoretical expectation that Mn remains at Mn^{4+} during the electrochemical charge and discharge. However upon careful inspection, subtle but certain differences among samples can been resolved. First of all, both peaks 1 and 2 shift to lower energy with the increase of SOC (sample A being at lowest energy) in both IPFY and TEY modes. Apparently TEY mode presents more clear change with the appearance and the shift of the shoulder peak "a" along with the shift of peaks 1 and 2 as a function of SOC. These observations, especially the existence of peak "a", could mean an increase of Mn with lower oxidation state (Mn^{2+} or Mn^{3+})[22] with charge. However the existence of Mn^{2+} and Mn^{3+} in LNMO with SOC of 40% and above is contradictory to the stable oxidation state at Mn^{4+}, predicted from the open-circuit energy diagrame of LNMO[1]. Similar Mn L-edge XANES evolution in Li_2MnO_3 with different SOCs has been assigned to the electronic structure change at the oxygen site with the assistance of theoretical calculation[13]. That work revealed that the electronic state of oxygen ion (oygen ion loses electrons) in Li_2MnO_3 can cause the Mn $L_{3,2}$-edge shifting to lower energy and the increase of the peak 2. Additionally, peak "a" is much better resolved in TEY for all samples, the increased intensity of peak "a" could be due to the surface reconstruction[14,20,27] in LNMO after cycling. It should be mentioned that the surface of cycled LNMO is very complex, though the current spectroscopic change might be caused by the oxygen structural change being analogous to that of Li_2MnO_3, we cannot completely rule out the surface Li enrichment as being discussed in the Ni XANES section. Such Li concentration gradient has been widely observed in several metal oxide cathodes and is a consequence of lithium diffusion[6, 14] and/or structural modification[20]. It should also be pointed out that regardless of the causes for the spectroscopic difference, oxygen structural change or the possible surface Li enrichment, this modification shall be constrained in a very small region considering the probing depth of less than 5 nm at TEY mode. In comparison, there are very small spectroscopic difference in IPFY as shown in Fig. 3a. Furthermore, it can be observed that Mn in LNMO with SOC of 0% is different from the pristine one especially on the surface in which peak 1 of the cycled one appears at lower energy relative to that in the pristine one (see Fig. 3b). This subtle chemical shift on the surface of LNMO indicates that the change in surface structure after charge/discharge cycles shall be responsible for the activation (cycle 2 has much better electrochemical performance than the first charge/discharge cycle) as a result of improved Li ion diffusion and electronic conductivity. Finally, it is obvious that the Mn L_3-edge variation as a function of SOC (Fig. 3b) is not as systematic as that of Ni L_3-edge in Fig.2 (Fig. 2a), which highlights the different role of Ni and Mn in the electrochemical process of LNMO.

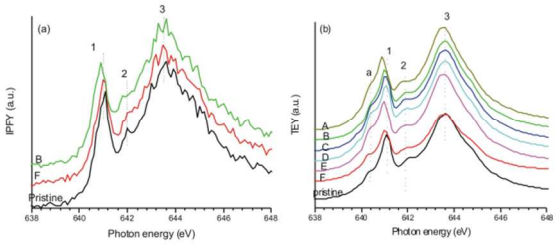

Fig. 3 Mn L_3-edge XANES of LNMO with different SOC and pristine LNMO in IPFY (a) and TEY modes (b).

Finally, the electronic structure of LNMO with different SOC was examined by O K-edge XANES to glean an insight of the role of oxygen in the lithiation process as shown in Fig. 4. The O K-edge arises from excitations of O 1s electron to the

unoccupied orbitals with dominant p character. Peaks a and b arise from the hybridization of O 2p and metal (Ni and Mn) 3d orbitals and the broad peaks at c and d are due to hybrid states of O 2p with metal 4sp characters. Upon the increase of SOC four spectroscopic changes can be observed: a shift of peak "a" to lower energy; a broadening of peaks "c" and "d"; a shift of peaks "c" and "d" to higher energy; and an increase of relative ratio of peaks ("a", "b") to the broad peaks ("c" and "d"). These changes are apparent in both Fig. 4a and 4b, while more obvious in bulk sensitive FY mode. It is known that the shift of peak "a" to lower energy is due to a higher oxidation metal state because of the greater effective nuclear charge[12]. This is consistent with the Ni $L_{3,2}$-edge results that with higher SOC Ni is more oxidized. Peaks "c" and "d" are due to the σ* state in ligand K-edge XANES and the σ* state is sensitive to the bond distance[23, 24]. Shorter metal-ligand distance will cause an energy shift to higher which is the case in this study when the SOC increases. This suggests that the extraction of Li ion shall reduce the transition metal-oxygen bond length. It has been established[25] that an increase of peaks ("a","b") over to the broad peak ("c", "d") represents an increase of metal-oxygen hybridization. This agrees with the conlusion of a shorter metal-oxygen bond length mentioned above. Fig.4 also clearly presents the surface and bulk difference at O site. First of all, surface has much smaller peak "a" shift with the increase of SOC which could indicate a less oxidized Ni than that in the bulk and again agrees with the Ni L-edge results. Furthermore, at the bulk, LNMO with higher SOC have lower intensity at peaks "c" and "d" than the pristine one does, except LNMO with 0% SOC which has very similar O feature to that of pristine LNMO; in contrast, at the surface cycled ones have much intense peak "c" and "d" than the pristine one. Since a higher intensity in O K-edge XANES could mean more unoccupied O 2p states; thus this agrees with above assumption of electron lose at oxygen side on the cycled LNMO surface which changes the Mn L-edge features. Interestingly, the extremely intense peak c in 0%SOC LNMO has previously been observed in lithiated anatase TiO_2 which has been attributed to a focusing effect due to a linear O-Li-O arrangment[11]. Those surface and bulk spectroscopic differences highlight the surface structure modification after several charge/discharge cycles and clearly indicate the contribution of oxygen in the electrochemical (de)lithiation process. We note that the relative intensity of peak c in cycled LNMO dcreases along the increase of SOC. This phenomenon might be cuased by the thicker SEI layer[26] in LNMO samples with higher SOC which may "block" oxygen signal from cycled LNMO to certain extent.

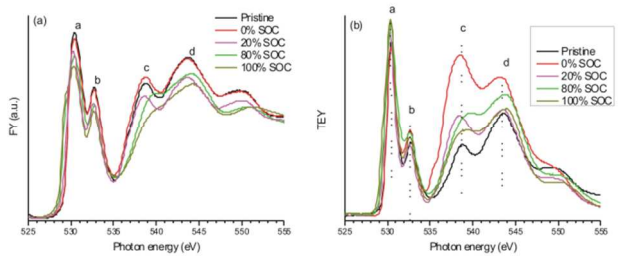

Fig.4 O K-edge XANES of LNMO with different SOC and pristine LNMO at FY (a) and at TEY modes (b).

In summary, detailed electronic structure at the Ni, Mn, and O sites in charged LNMO samples with different SOC along with the pristine LNMO has been studied by comprehensive XANES involving mutliple elements and edges in both surface and bulk sensitive modes. Spectroscopic evidence of the existence of Ni^{4+}, Ni^{3+} and Ni^{2+} in LNMO with different SOC has been found. Although Ni is the major redox species in charge compensation as expected, O is also actively involved in the process with non-trivial roles. The spectroscopic difference between surface and bulk in cycled LNMO observed at Ni, Mn and O sites implies the Li enrichment or a more oxidized oxygen ion on the surface after charge/discharge cycles. Different surface structure between fully discharged LNMO and pristine one as indicated by their Mn L_3-edge and O K-edge TEY spectra shall be responsible for the electrochemical activation in the first several cycles. These observations are useful for better understanding of this complicated spinel cathode and for its further development, especially when combined with theoretical calculation and modelling.

Notes and references

Thank Drs. J. Dynes and T. Regier at CLS for technical assistances. CLS is supported by NSERC, NRC, CIHR and the University of Saskatchewan. This work was supported by the National Natural Science Foundation of China (. 51272051), and Academic Expert Program of Harbin (RC2012XK017008).

[a] *Canadian Light Source Inc, Saskatoon, Canada. Fax: 1-306-6573535; Tel: 1-306-657-3587; E-mail: jigang.zhou@lightsource.ca*
[b] *School of materials engineering, Harbin Institute of Technology, China, htfang@hit.edu.cn*
[c] *School of chemical engineering, Harbin Institute of Technology, China*
[d] *Shanghai Institute of Microsystem and Information Technology, Chinese Academy of Science*

† Footnotes should appear here. These might include comments relevant to but not central to the matter under discussion, limited experimental and spectral data, and crystallographic data.

Electronic Supplementary Information (ESI) available:. See DOI: 10.1039/c000000x/

1. D. Liu, W. Zhu, J. Trottier, C. Gagnon, F. Barray, A. Guerfi, A. Mauger, H. Groult, C. M. Julien, J. B. Goodenough and K. Zaghib, *RSC Adv*, 2014, **4**, 154-167.
2. J. Song, D. W. Shin, Y. Lu, C. D. Amos, A. Manthiram and J. B. Goodenough, *Chem. Mater.*, 2012, **24**, 3101-3109.
3. J. Xiao, X. Chen, P. V. Sushko, M. L. Sushko, L. Kovarik, J. Feng, Z. Deng, J. Zheng, G. L. Graff, Z. Nie, D. Choi, J. Liu, J.-G. Zhang and M. S. Whittingham, *Adv Mater.*, 2012, **24**, 2109-2116.
4. N. P. W. Pieczonka, Z. Liu, P. Lu, K. L. Olson, J. Moote, B. R. Powell and J.-H. Kim, *The J.Phys.Chem. C*, 2013, **117**, 15947-15957.

5. G. B. Zhong, Y. Y. Wang, Y. Q. Yu and C. H. Chen, *J. Power Sources*, 2012, **205**, 385-393.
6. X. Liu, J. Liu, R. Qiao, Y. Yu, H. Li, L. Suo, Y.-s. Hu, Y.-D. Chuang, G. Shu, F. Chou, T.-C. Weng, D. Nordlund, D. Sokaras, Y. J. Wang, H. Lin, B. Barbiellini, A. Bansil, X. Song, Z. Liu, S. Yan, G. Liu, S. Qiao, T. J. Richardson, D. Prendergast, Z. Hussain, F. M. F. de Groot and W. Yang, *J. Am. Chem. Soc.*, 2012, 2012, **134**, 13708-13715.
7. J. G. Zhou, J. Wang, Y. F. Hu, T. Regier, H. L. Wang, Y. Yang, Y. Cui and H. J. Dai, *Chem.Comm.*, 2013, **49**, 1765-1767.
8. J. B. Goodenough and Y. Kim, *Chem.Mater.*, 2009, **22**, 587-603.
9. H. Wadati, D. G. Hawthorn, T. Z. Regier, G. Chen, T. Hitosugi, T. Mizokawa, A. Tanaka and G. A. Sawatzky, *Appl. Phys. Lett.*, 2010, **97**, 022106.
10. J. G. Zhou, J. Wang, L. Zuin, T. Regier, Y. F. Hu, H. L. Wang, Y. Y. Liang, J. Maley, R. Sammynaiken and H. J. Dai, *Chem. Chem. Phys.*, 2012, **14**, 9578-9581.
11. J. G. Zhou, H. T. Fang, J. M. Maley, M. W. Murphy, J. Y. Peter Ko, J. N. Cutler, R. Sammynaiken, T. K. Sham, M. Liu and F. Li, *J. Mater. Chem.*, 2009, **19**, 6804-6809.
12. W.-S. Yoon, M. Balasubramanian, K. Y. Chung, X.-Q. Yang, J. McBreen, C. P. Grey and D. A. Fischer, *J.Am. Chem. Soc.*, 2005, **127**, 17479-17487.
13. K. Kubobuchi, M. Mogi, H. Ikeno, I. Tanaka, H. Imai and T. Mizoguchi, *Appl. Phys. Lett.*, 2014, **104**, 053906.
14. X. Liu, D. Wang, G. Liu, V. Srinivasan, Z. Liu, Z. Hussain and W. Yang, *Nat Commun*, 2013, **4**. 2568-2566
15. W. Wang, J. Zhang, Z. Jia, C. Dai, Y. Hu, J. Zhou and Q. Xiao,*Phys.Chem.Chem.Phys.*,2014.DOI:10.1039/c3cp55495c
16. Y. Y. Liang, Y. G. Li, H. L. Wang, J. G. Zhou, J. Wang, T. Regier and H. J. Dai, *Nat. Mater.*, 2011, **10**, 780-786.
17. J. Wang, J. Zhou, Y. F. Hu and T. Regier, *Energ. Environ.Sci.*, 2013, **6**, 926-934.
18. A. J. Achkar, T. Z. Regier, H. Wadati, Y. J. Kim, H. Zhang and D. G. Hawthorn, *Phys. Rev. B*, 2011, **83**, 081106.
19. H. X. Wang, C. Y. Ralston, D. S. Patil, R. M. Jones, W. Gu, M. Verhagen, M. Adams, P. Ge, C. Riordan, C. A. Marganian, P. Mascharak, J. Kovacs, C. G. Miller, T. J. Collins, S. Brooker, P. D. Croucher, K. Wang, E. I. Stiefel and S. P. Cramer, *J.Am. Chem. Soc.*, 2000, **122**, 10544-10552.
20. S. Hy, W.-N. Su, J.-M. Chen and B.-J. Hwang, *J. Phys. Chem. C*, 2012, **116**, 25242-25247.
21. M. Matsui, K. Dokko and K. Kanamura, *J.Electrochem. Soc.*, 2010, **157**, A121-A129.
22. K. A. Stoerzinger, M. Risch, J. Suntivich, W. M. Lu, J. Zhou, M. D. Biegalski, H. M. Christen, Ariando, T. Venkatesan and Y. Shao-Horn, *Energ. Environ. Sci.*, 2013, **6**, 1582-1588.
23. J. G. Zhou, X. T. Zhou, R. Y. Li, X. L. Sun, Z. F. Ding, J. Cutler and T. K. Sham, *Chem.Phys. Lett.*, 2009, **474**, 320-324.
24. Y. H. J. Zhou, X. Li, C. Wang, L. Zuin, *RSC Adv.*, 2014.
25. J. G. Chen, *Surf. Sci. Rep.*, 1997, **30**, 1-152.
26. M. Matsui, K. dokko, and K. Kanamura, J. Electrochem. Soc., 2010, 157(2) A121-A129
27. F. Lin, I. Markus, D. Nordlund, T. Wang, M. Asta, H. Xin, M. Doeff, Nat. Commun. 2014, DOI:10.1038/ncomms4529